

Measuring Neutron Absorption Cross Sections of Natural Platinum via Neutron
Activation Analysis

By
Nick Petersen

A thesis submitted to
Oregon State University
Department of Physics
Corvallis, Oregon

In partial fulfillment
of the requirements for
the degree of

Bachelor of Science

Presented June 11, 2012

Commencement June 17, 2012

Abstract:

This thesis presents a measurement of the resonance integral and thermal cross section – which together represent the total neutron absorption cross section – of the naturally occurring isotopes of platinum that emit gamma radiation upon neutron absorption. The measurements were made via neutron activation analysis. Platinum samples were bombarded by neutrons produced in Oregon State University's TRIGA nuclear reactor. Afterwards, the decay of the excited samples was measured to determine the activity of each isotope, yielding measurements of the cross sections for each. This experiment was repeated multiple times in different reactor locations to improve accuracy.

Previous measurements of these values have been flawed by poor photon detector resolution, and evolving branching ratios, half-lives, natural abundances. A search of the literature reveals poor agreement and large error estimations.

The results from this thesis are consistent, with one exception: there appears to be a systematic disagreement between the resonance integral measurements of samples bombarded in two different reactor locations. This discrepancy has now been seen in several experiments, which indicates inconsistent epithermal flux throughout OSU's reactor.

TABLE OF CONTENTS

1 INTRODUCTION	1
• 1.1 MOTIVATION	1
• 1.2 CROSS SECTION AND NEUTRON ENERGY	2
• 1.3 DECAY SCHEME AND NUCLEAR SPIN	5
• 1.4 PLATINUM ISOTOPES	6
2 EXPERIMENTAL METHODS	8
• 2.1 EXPERIMENT OVERVIEW.....	8
• 2.2 INDEPENDENT EXPERIMENTS	8
• 2.3 FLUX MONITORS.....	11
• 2.4 CAPTURE OF GAMMA SPECTRA	11
• 2.4 DATA ANALYSIS	12
• 2.5 DETECTOR EFFICIENCY.....	14
3 RESULTS	16
• 3.1 CLICIT RESULTS.....	16
• 3.2 CADMIUM-ENCLOSED RABBIT RESULTS	17
• 3.3 NON CADMIUM-ENCLOSED RABBIT RESULTS.....	19
• 3.4 THERMAL COLUMN RESULTS	20
• 3.5 UNCERTAINTY CALCULATIONS.....	21
4 DISCUSSION	22
• 4.1 PREVIOUS RESULTS	22
• 4.2 PT-190 → PT-191 CROSS SECTION	23
• 4.3 PT-194 → PT-195M CROSS SECTION	24
• 4.4 PT-196 → PT-197G CROSS SECTION.....	24
• 4.5 PT-196 → PT-197M CROSS SECTION	24
• 5.6 PT-198 → PT-199G CROSS SECTION.....	24
5 CONCLUSION	26
6 ACKNOWLEDGEMENTS	27
7 REFERENCES	28

1 INTRODUCTION

1.1 Motivation

The neutron absorption cross sections of the naturally occurring isotopes of Pt (190, 192, 194, 196, 198) have not been adequately measured. Some of the values have been published in the literature only once or twice, and some of these measurements were done in the 1970s or earlier when technology (specifically photon detectors) was simply not good enough to do cross section measurements with a reasonable degree of accuracy. For example, the epithermal cross section (resonance integral) for neutron capture of Pt-198 to the metastable state of Pt-199 has been presented only twice in the literature and the average of the two is smaller than their standard deviation. See Tables 9 and 10 in Section 4.1 for more literature values. This thesis presents a methodical measurement of the neutron absorption cross sections of all natural Pt isotopes that produce radioisotopes following neutron capture (190, 194, 196, 198).

Pt is noteworthy for the fact that when two of the stable isotopes (196 and 198) absorb a neutron, each product (197 and 199 respectively) has two possible product nuclei: a ground state and a more highly excited metastable state. The ground state of Pt-197 has a nuclear spin of $1/2$ while the ground state of Pt-199 has nuclear spin of $5/2$. In both cases, the excited metastable state product has a nuclear spin of $13/2$. The ground and metastable states have different half-lives and emit different energy gamma rays upon decay, so the thermal neutron absorption cross section and epithermal resonance integral are considered separate for each state, even though the parent nucleus is the same.

Pt-195 also has metastable and ground states with spins of $13/2$ and $1/2$ respectively. However, the ground state is stable and therefore cannot be probed with neutron activation analysis. Only the metastable state of Pt-195 was measured.

For this experiment, the metastable state of Pt-199 could not be measured due to its extremely short half-life (13.6 s). It proved impossible to retrieve the samples and place them in front of a detector fast enough to record meaningful data. Also, the reaction $\text{Pt-192} \rightarrow \text{Pt-193}$ was not measured because Pt-192 has an extremely low natural abundance and Pt-193 emits very few characteristic gamma rays.

Pt is also a noteworthy element because the (admittedly flawed) current literature suggests that Pt-190 has an epithermal cross section of a smaller value than the thermal cross section. This is highly unusual, as almost all nuclides have larger epithermal cross sections than thermal, usually an order of magnitude larger. It is important to verify these results to improve our understanding of nuclear systematics.

1.2 Cross Section and Neutron Energy

The nuclear cross section is used to characterize the probability of a nuclear interaction with incident radiation. It has dimensions of area and is usually measured in units of barns, where 1 b is equal to 10^{-24} cm². A larger cross sectional area means the effective nuclear area that incoming radiation sees is larger, making the probability of interaction greater. It can be used to describe the probability of absorption, elastic scattering, inelastic scattering, or the total of all three. In this paper, we are interested only in characterizing the probability of neutron absorption with subsequent emission of gamma rays; henceforward the neutron absorption cross section will simply be referred to as the “cross section.”

The cross section is a function of specific nuclear characteristics and incident neutron energy. Slower neutrons with kinetic range in the range of 0 to 1 eV are referred to as thermal neutrons. Neutrons that have more kinetic energy, in the range of 1 eV to about 10 keV are called epithermal neutrons. Although the cross section is a continuous function of neutron energy, the cross section function behaves differently for thermal and epithermal neutrons.

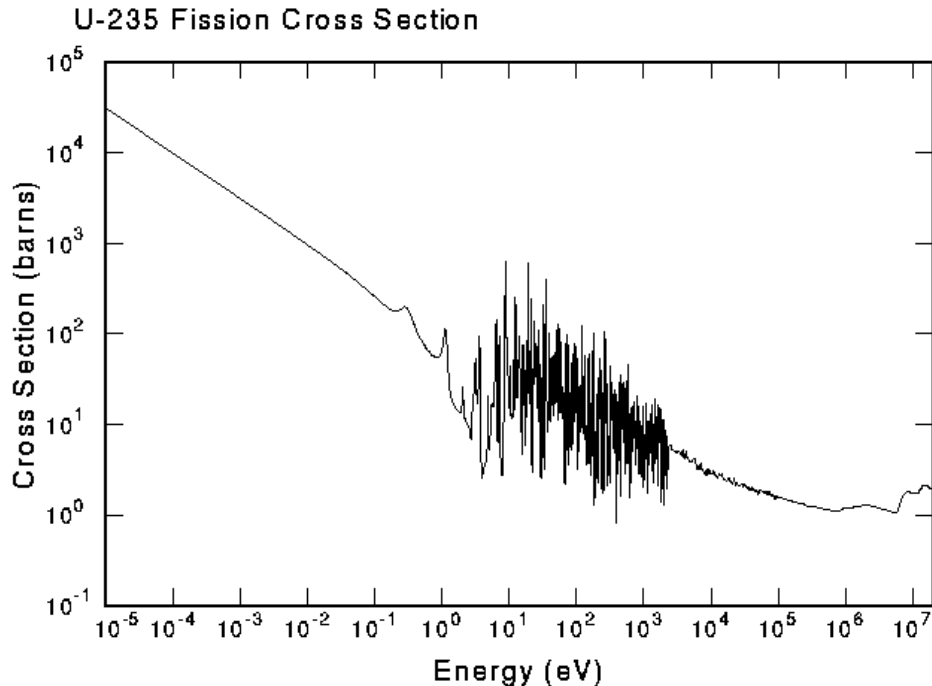


Figure 1: A neutron absorption cross section for U-235 is shown to illustrate the general form of the cross section as a function of energy. Data of this type have never been adequately measured for Pt nuclei, but they are expected to display similar behavior. [1]

As shown in Figure 1, the log-log plot of cross section vs. neutron energy is linear for thermal neutrons. Thermal cross section plots for all nuclei have the same slope – which is inversely proportional to the speed of the incident neutron – so the thermal cross section of any nuclide can be characterized by a single intercept. It is conventional to represent the cross section at the value 0.025 eV, which is the peak of Maxwell-Boltzmann energy distribution. Given this value, the thermal cross section for neutrons of any energy can be easily calculated.

Figure 1 also shows that in epithermal range, the cross section becomes very unpredictable, with certain energies resonating with the target nuclei and certain energies having very little likelihood of interacting. The specific measurement of these resonance peaks is extremely difficult, as the energy of incident neutrons would have to be restricted to very small ranges. This is outside the scope of our experiment. In order to characterize the cross section of this resonance region, we use the resonance integral. This is the total integral of the cross section over the entire epithermal neutron energy range. It essentially provides the average cross section for epithermal neutrons. Henceforward, the epithermal cross section will simply be referred to as the resonance integral.

In order to make this measurement, the flux of epithermal neutrons must be known. For all fission reactors, this value is proportional to $E^{-(1+\alpha)}$, where α is a small constant that accounts for the geometry and physical characteristics of each individual reactor. For this experiment, we make the assumption that $\alpha=0$, so that the flux is proportional to E^{-1} .

The general differential reaction rate equation governing a particle population is given by Equation 1:

$$dN = Rdt - \lambda NdT \quad (1)$$

where R is the number of particles added to the population N . In this case R is the number of nuclei that absorb thermal or epithermal neutrons, which is given by Equation 2:

$$R = N_0(\sigma\phi_{th} + I\phi_{epi}) \quad (2)$$

where N_0 is the number of target nuclei of interest, σ is the thermal cross section, I is the resonance integral, ϕ_{th} and ϕ_{epi} are the thermal and epithermal neutron fluxes respectively, and λ is the decay constant of the activated nucleus.

Integrating Equation 1 yields the total of number of activated nuclei at time t . This is given by Equation 3 below:

$$N(t) = \frac{R}{\lambda}(1 - e^{-\lambda t_i})e^{-\lambda t} \quad (3)$$

where t_i is the total time of neutron bombardment. Finally, putting Equations 2 and 3 together yields the formula for the activity of the sample at a given time, as given by Equation 4:

$$a(t) = N_0(\sigma\phi_{th} + I\phi_{epi})(1 - e^{-\lambda t_i})e^{-\lambda t} \quad (4)$$

This equation has two unknowns – σ and I – so it is impossible to solve. In order to generate more equations, the bombardment can be run multiple times with different levels of ϕ_{th} and ϕ_{epi} .

The vast majority of neutrons encountered in typical applications (experiments, commercial power, etc.) lie in either the thermal or epithermal range. For example, the number of fast neutrons produced by a nuclear fission reactor – and the number that interact – is relatively very small. The cross section for fast neutrons is also extremely small. Both of these factors mean that fast neutrons

can be neglected. Therefore, the cross section for a given nuclei – which is a continuous function of energy – can be represented by two values: the thermal cross section and the resonance integral.

1.3 Decay Scheme and Nuclear Spin

A sample decay diagram of a generic neutron activated Pt isotope is shown in Figure 2. After absorbing a neutron, the excited nucleus will emit a cascade of primary and secondary gamma rays, eventually ending up in either the ground state or the metastable state (if it exists). Photons usually prefer to carry only one or two units of angular momentum, which is why two (or more) of these gamma rays are required to reach the metastable or ground state. These primary and secondary gamma rays are referred to as “prompt” because they are emitted by an activated nucleus immediately after neutron absorption (on the order of picoseconds) and therefore cannot be measured in our experiments.

Nuclei that end up in the metastable state after emission of prompt gamma rays can emit more photons, which will again carry some of the nucleus’s spin, sending into the ground state. This process is the normal decay of the metastable state, so it is governed by the characteristic half-life and can therefore be counted to determine the activity of the state. Metastable nuclei can also beta-decay, becoming an unstable isotope of Au. Although the beta electrons cannot be measured by our detectors, the characteristic decay photons of each Au isotope are measured and also used to calculate the metastable activity.

Neutron activated Pt can also move directly to the ground state after prompt gamma ray emission. Nuclei will also beta decay to unstable Au, which can then be measured. When calculating the activity of the ground state, nuclei arriving from the metastable state via isomeric transition must be subtracted out.

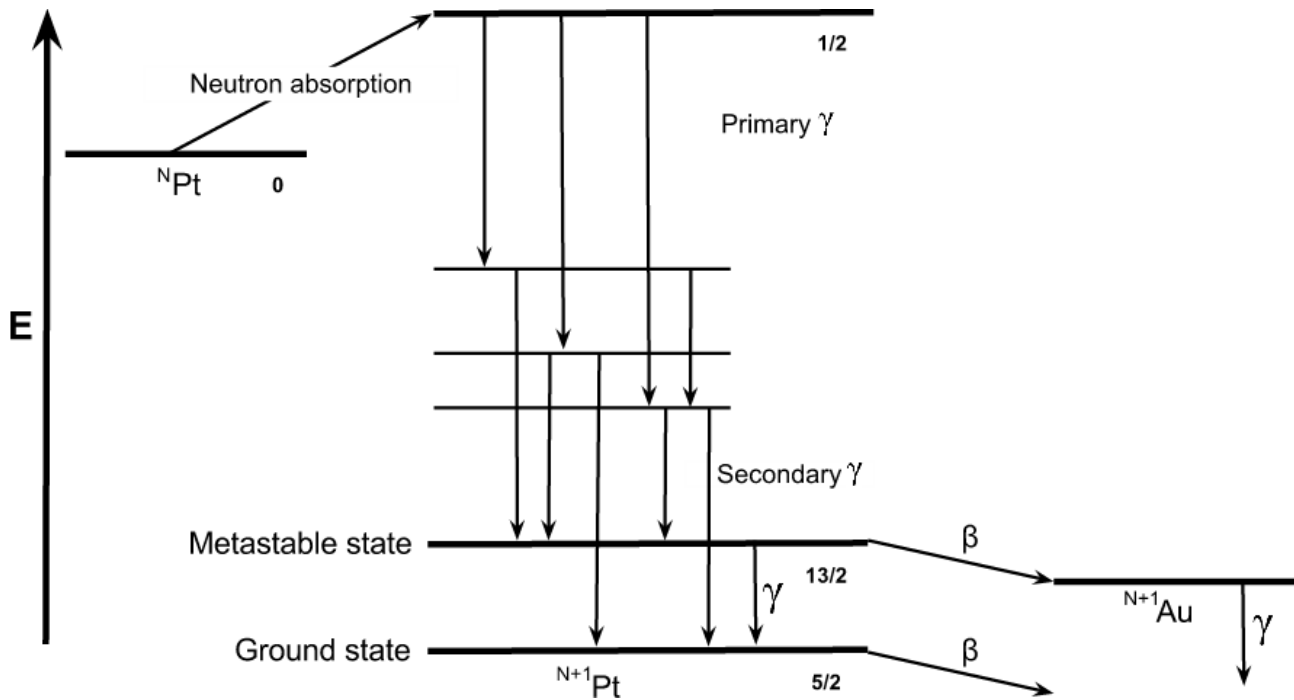


Figure 2: A sample decay scheme for neutron absorption by a Pt nucleus. This is a generic representation and does not illustrate the decay scheme for any particular isotope. Note that the metastable state does not exist for all Pt isotopes.

1.4 Platinum Isotopes

Platinum has six naturally occurring stable isotopes, five of which emit gamma rays upon irradiation. It is cross sections of these five isotopes that we measured in the experiment. Pt-197 and Pt-199 both have two possible spin states that are considered separately. Table 1 shows all the interactions considered in this experiment.

Target Nuclei	Natural Abundance	Atomic Mass	Product of Absorption	Half-Life (s)	γ Energy (keV)	Branching Ratio
Pt-190	0.00014	189.96	Pt -191	248832	538.91	0.137
					409.476	0.08
					359.927	0.06
Pt-192	0.0782	191.961	Pt-193	374112	135.5	0.0011
Pt-194	0.32967	193.963	Pt-195	346464	98.883	0.114
					129.765	0.028
Pt-196	0.25242	195.965	Pt-197g	71856	77.343	0.171
					192.362	0.037
					268.705	0.00231
			Pt-197m	5724	346.81	0.111
					279.11	0.023
Pt-198	0.07163	197.968	Pt-199g	1848	542.963	0.117
					493.74	0.0447
					317.061	0.0388
			Pt-199m	13.6	391.93	0.85

Table 1: Information about each Pt isotope considered in the experiment. Pt-196 and Pt-198 both have two different possible nuclear spin states upon neutron absorption. Most of these excited nuclei emit multiple gamma rays with sufficient branching ratios to measure. Atomic abundances from [2], branching ratios from [3].

Due to the nuclear characteristics of each isotope, they will each have unique cross sections. Pt-196 and Pt-198 both have separate probabilities of ending up in ground or metastable states after neutron absorption, so the cross section for those are considered separately as well.

2 EXPERIMENTAL METHODS

2.1 Experiment Overview

99.99% pure, natural samples of Pt foil with thickness 0.025 mm were used in these experiments. The samples were irradiated with neutrons in Oregon State University's Training, Research, Isotopes, and General Atomics (TRIGA) Reactor. Natural Pt was used because it contains each naturally occurring isotope of Pt. A random sample of natural Pt has the normal abundance of each isotope within a given error. Upon absorption of neutrons, each nucleus becomes an unstable isotope. Upon decay, unstable nuclei of each type emit unique gamma rays of known energy and branching ratio. By measuring these gamma rays, we can calculate the activity of each nuclei type after neutron bombardment. Since the number of original Pt nuclei of each type was known before bombardment, we can determine the number of neutrons absorbed, and hence the cross section. Performing the experiment multiple times allows us to measure the thermal cross section and resonance integral – both components of the overall cross section – independently. Multiple runs also improve the statistics of our results.

2.2 Independent Experiments

Four different samples of varying mass were used to perform four separate experiments in different reactor facilities. There were several constraints on the masses chosen. The upper limit of each mass was determined by safety concerns and the need to limit dead time in the detector (see Section 2.4). For safety, masses were chosen so that the activity after absorption would not exceed roughly 200 μCi . The lower limit was bounded by the fact that the least active isotope needs to have about 10^4 total counts to be statistically significant, otherwise the error would be too great. Each mass was different because the expected reactor fluxes were different. The masses were chosen for each experiment with a rough estimate of the activity (using Equation 4). Once an activity estimate was made, samples were cut out of pure Pt foil. For the TC and Rabbit experiments, the masses were plastic in polyethylene cylindrical capsules and heat sealed to reduce the possibility of spilling material inside the core, whereas the samples for the CLICIT experiment was sealed inside a quartz container. The masses used in each run are shown in Table 2, along with general information about each run.

	Thermal Flux	Epithermal Flux	Pt sample mass (mg)	Irradiation time	Delay before analysis
CLICIT	0	1.17E12	11.6	1 h	2.24 h
TC	8.5E10	2.0E8	46.4	2 h	3.19 h
Rabbit	8.5E12	3.5E11	12.1	5 min	15.32 min
Rabbit + Cd	0	3.5E11	13.9	3 min	14.97 min

Table 2: Displays the neutron flux provided by each facility, the masses of the samples used in each experiment run, irradiation time, and elapsed time between completion of irradiation and beginning of analysis.

Each run was done in a different facility of the reactor so that the levels of thermal and epithermal neutron flux would vary, allowing us to use Eq. 1 with more degrees of freedom. The four facilities are: the cadmium-lined in-core irradiation tube (CLICIT), the thermal column (TC), the fast pneumatic transfer facility ("rabbit") and the cadmium enclosed rabbit. The CLICIT and rabbit facilities are shown in Figure 3. Cd-113 – a stable cadmium isotope – has an extremely high total cross section (including scattering and absorption interactions) for thermal neutrons only. As a result, CLICIT and the cadmium lined rabbit facilities block virtually all thermal neutrons during irradiation, which allows us to measure the Pt resonance integrals more directly. When the thermal flux is zero, the activity equation (Equation 4) becomes a function of a single variable, meaning the calculation of the resonance integral is not dependent on the calculation of the thermal cross section.

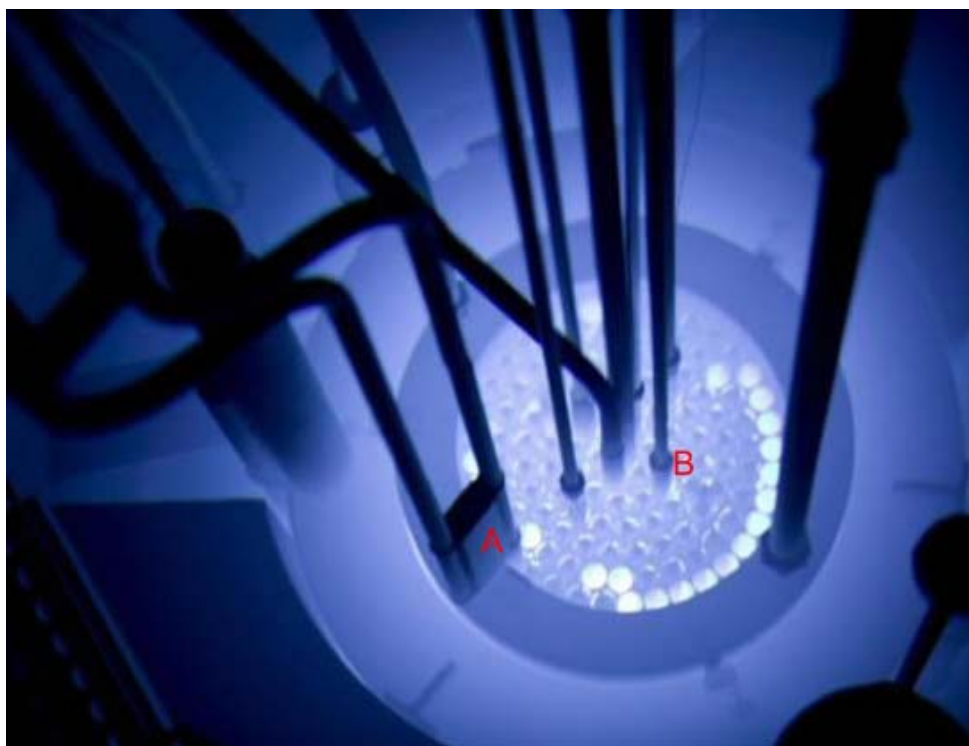


Figure 3: OSU's TRIGA reactor core is shown from above. The illumination is from Cerenkov radiation. The rabbit facility is labeled as (A). The incoming and outgoing pneumatic tubes can be seen. The CLICIT is labeled (B). It inserts the sample directly into a vacant fuel rod tube. The TC is located further away and is not shown. [4]

The rabbit facility is different from the others because it allows for measurement of sample activity very quickly after irradiation. Since it uses a pneumatic sample transfer system that we operate ourselves, we can retrieve the rabbit samples seconds after irradiation. Then we can personally take the samples directly to the lab for analysis, which takes around 15 minutes.

For each reactor location, multiple runs were performed (at each distance from the detector). Each run usually provided multiple measurements of two or three isotopes. All of these results were averaged together to create the final result. Certain outlier measurements were left out of the average if they had a high χ^2 value, which is an indication that the decay of the sample activity does not fit with the half-life of the isotope listed in the literature. This usually means that there was some other source of gamma rays with a similar energy, making it impossible to use those data to calculate activity.

2.3 Flux Monitors

Each sample was irradiated alongside Au and Co flux monitors. These elements were chosen because their cross sections and resonance integrals have been very accurately established, due to their useful applications in a variety of fields. By measuring the gamma activity of the flux monitors after irradiation, the total of both the thermal and epithermal fluxes incident on the Pt samples can be accurately calculated. As can be seen in Table 3, the Co and Au both have adequately long half-lives that they did not interfere with the activity measurements of the Pt. The flux monitors were left in storage while the Pt samples were measured with the detector. After the Pt was adequately measured, the Co and Au flux monitors were still active enough to measure with the detectors.

Isotope	Activated State	Half-Life
Au-197	Au-198	2.7 d
Co-59	Co-60	5.27 y

Table 3: Information for both flux monitor elements.

2.4 Capture of Gamma Spectra

The gamma detectors used in this experiment were of nitrogen-cooled, germanium crystal type. The germanium crystals used in the detectors are extremely expensive, but they allow a very high resolution in the energy spectra of incoming radiation. Without this resolution, it would be exceedingly difficult to calculate the cross sections accurately. Each time incident gamma radiation is absorbed by the detector, it creates numerous electron-hole pairs. The number of electron-hole pairs is proportional to the energy of the absorbed gamma ray. Then the detector sweeps out the electron-hole pairs, creating a pulse with an RC time-constant tail. The amplifier increases the voltage of the signal and cuts the RC tail from the signal, which is then sent to the computer. It interprets each incoming pulse as a single gamma capture whose energy is proportional to the amplitude of the signal.

While the electron-hole pairs are being swept out, the detector is not able to detect any more incident radiation for a short time, even if it is absorbed by the germanium crystal. This is called "dead time." The exact dead time is recorded and accounted for in the data analysis (i.e. the calculations are adjusted due to the extra decay that occurs), but too much dead time can negatively impact the statistics of the experiment.

All the experiment runs were performed in the same manner. The rabbit runs were placed in front of the detectors almost immediately after irradiation. In accordance with reactor staff procedures, the samples placed in the other facilities (CLICIT and thermal column) were then put into storage for several more hours before they could be placed in front of a detector. The activity is related to the decay half-life, so the samples were initially hot due to the products with shorter half-lives like Pt-199g (30.8 minutes) and Pt-197m (19.96 hours). In order to decrease dead time due to the high activity of these specific nuclei, the samples were initially placed far away from the detector (25 cm). As time went on, the activity decreased, allowing us to move the samples closer to the detector to measure the products with longer half-lives without having to worry about dead time. We continued on in this manner, moving the samples closer to the germanium detector by 5 cm increments, measuring the counts and gamma ray spectra at each point. After several days in front of the detector, the Pt samples were adequately measured, allowing the Co and Au flux monitors to be placed in front of detectors and measured.

2.4 Data Analysis

To record the data, Ortec's MAESTRO software for Windows Model A65-B32 was used. MAESTRO counted each gamma incident on the detector and recorded its energy during a specified live time. To improve the statistics of the experiment, MAESTRO was programmed to automatically make multiple recordings of counts and gamma spectra at each position. After recording multiple runs in series, the measured sample activity was averaged, giving better results. As shown in Figure 1, all of the isotopes except Pt-193 emit multiple gamma rays with significant branching ratios, meaning that the activity of single isotope can be measured multiple times for each sub-run.

Each gamma peak of interest was manually selected in MAESTRO. The program subtracted out the background, then provided an area of the peak (total number of counts minus the projected background counts) and an uncertainty. All of these data were moved to Excel for analysis. The counts for a known live time were used to calculate the reaction rate for each sub run, which were averaged together. This average was used to find the activity of the sample and therefore the resonance integral and thermal cross section using Equation 4. The resonance integral for each isotope was measured first using the CLICIT and the cadmium-enclosed rabbit. Then the calculated resonance integral values were used to help find the thermal cross section.

A log plot of the first CLICIT run A count is shown in Figure 4. This was recorded over 7.85 min (real time) at a distance of 25 cm from the detector.

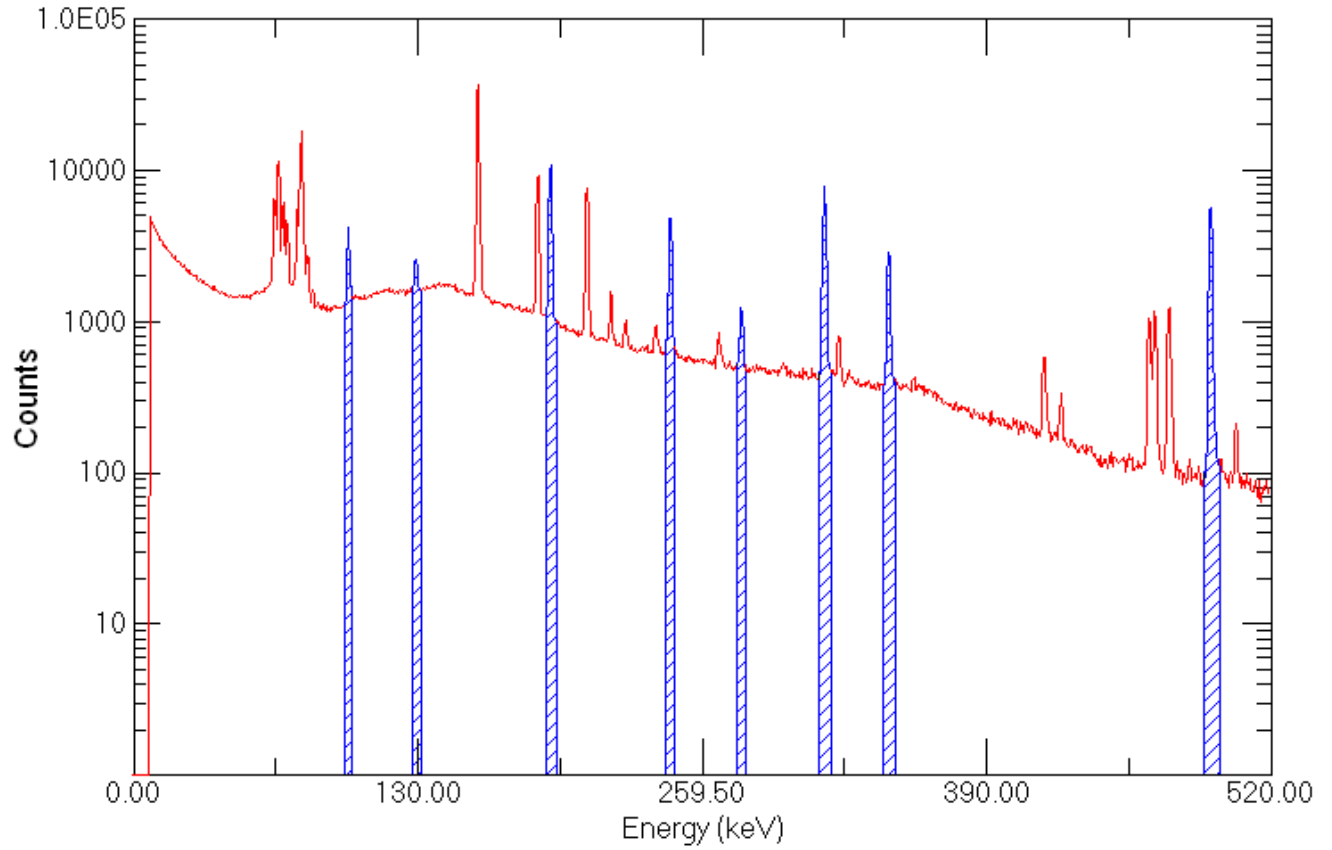


Figure 4: Log plot taken from MAESTRO. Regions of interest (ROIs) are labeled with blue.

After retrieving the number of counts, the adjusted counting rate R is calculated via Equation 5.

$$R = \frac{C \cdot e^{\Delta t \cdot \lambda} \cdot f}{t_L} \quad (5)$$

where C is the total number of counts, Δt is the elapsed time from the start of the counting run, f is a factor which corrects for the dead time, and t_L is the live time. Multiple counts are retrieved from the same distance from the detector – 12 different counts at 25 cm in the case of the CLICIT A run. The R value is calculated for each count and averaged together. This average R is used to calculate the activity a of the sample at the end of bombardment (EOB) via Equation 6:

$$a = \frac{\bar{R}}{e^{-\Delta t \cdot \lambda} \cdot B \cdot E} \quad (6)$$

where Δt is the elapsed time between the EOB and the beginning of the run, B is the branching ratio for the particular gamma decay, and E is the efficiency of the detector at that specific detector distance and gamma ray energy (see Section 2.5). Once the activity of the sample is known, the cross section of interest is calculated using the methods of Equation 4.

2.5 Detector Efficiency

The HPGe photon detector does not capture and record every photon of interest. We assume each activated nucleus is an isotropic source, so the vast majority of photons emitted by the activated aren't incident of the Ge crystal. In addition, some of the photons incident on the detector won't be absorbed, which depends on the photon energy.

In order to relate counts to the sample activity, an empirical calibration must be done to determine the detector efficiency. This is done by placing several samples of known activity in front of the detectors at the distances to be used in the experiment. Active Ba and Eu samples were used because their half-lives are well known and they emit photons at a variety of energies.

The calibration is done in a similar manner as the experiment described in Section 2.4, except the activity is already known, and the only value to be measured is the efficiency. Figure 5 shows a plot of the efficiency results at 15 cm as an example.

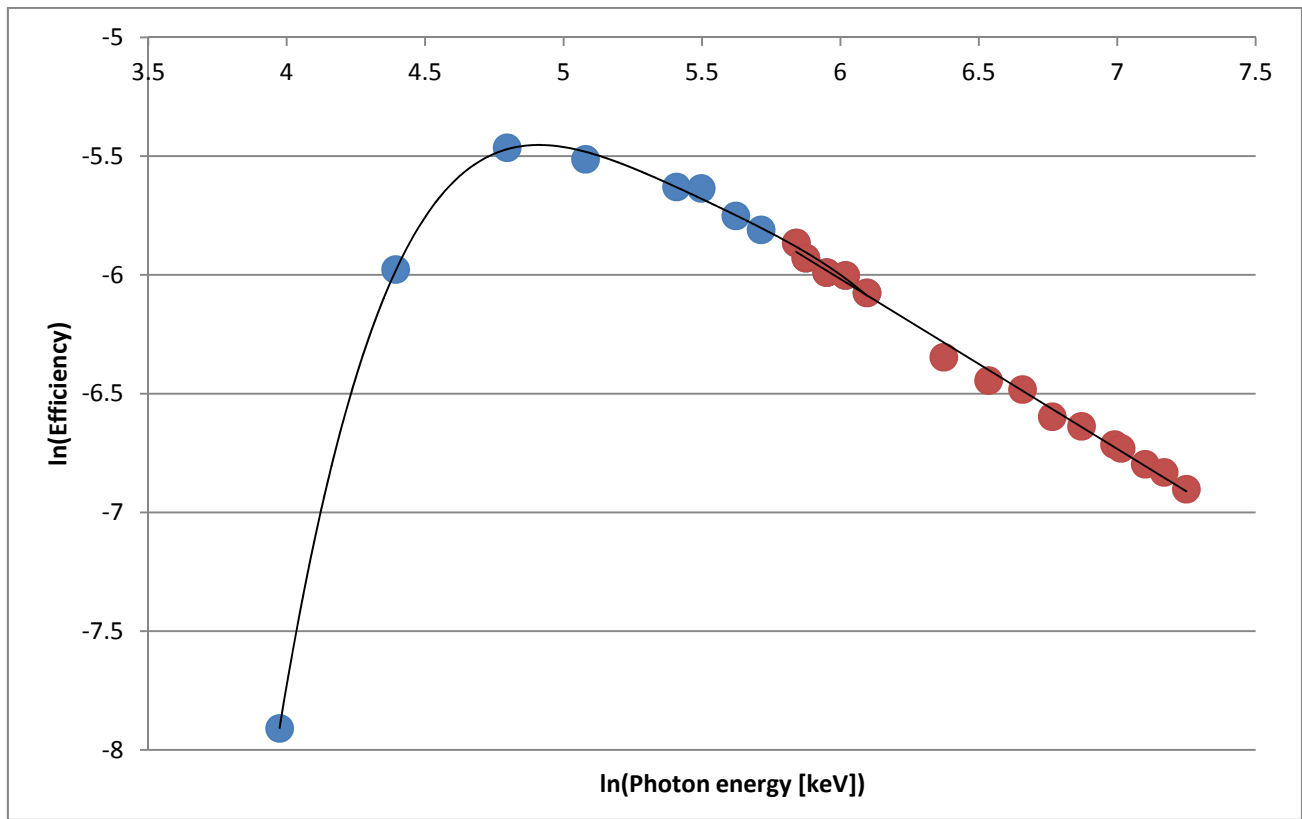


Figure 5: Natural log plot of detector efficiency vs. photon energy for samples located 15 cm away from the detector. The colors indicate regions with different equations of best fit. Data points represent values from both Ba and Eu photons of various energies

Two different best-fit equations are used. The natural log of the efficiency of photons with energy less than ~ 300 keV obey a fourth order polynomial fit, while the natural log of the efficiency of photons with energy greater than ~ 300 keV follows a linear relationship. Since the efficiency is only a property of the detector set up and photon energy, the appropriate efficiency for Pt photons will follow the same best-fit equations. This only applies for samples placed 15 cm away from the detector. Separate efficiency measurements were done for the other distances in the same manner, but in the interest of brevity they are not shown here.

3 RESULTS

3.1 CLICIT Results

The CLICIT location in the reactor is lined with cadmium, so virtually all thermal neutrons are absorbed. Therefore only the measurement of the resonance integral is made; the thermal cross section is irrelevant. These results are shown in Table 4.

The χ^2 distribution is a standard method of determining statistical significance. As the counts are made, the decay indicated by a specific gamma energy can be compared to what would be expected from a given half-life. A higher χ^2 value indicates a larger discrepancy between what is observed and what is expected. It most likely means that there is some background source of photons of the same energy that is skewing the results.

Interaction	Gamma (keV)	Run	Resonance Integral (Barns)	χ^2 /Degrees of Freedom	Weighted Average (Barns)
190 → 191	359.9	C	137.63	1.094	137.1 (244)
		D	135.07	1.356	
	456.5	C	138.41	0.106	
	538.91	C	130.02	1.394	
D		132.24	0.821		
194 → 195m	98.88	A	4.99	1.455	5.10 (32)
		B	5.14	0.660	
		C	5.21	19.496	
		D	5.21	28.783	
	129.77	A	5.30	0.428	
		B	5.42	0.945	
		C	5.45	3.295	
		D	5.41	2.603	
196 → 197g	192.36	B	8.40	0.865	8.52 (90)
		D	8.32	2.808	
	268.71	B	8.63	0.628	
		C	9.08	32.439	
196 → 197m	279.11	A	0.534	1.569	0.497 (22)
		B	0.539	1.067	
	346.81	A	0.468	1.667	
		B	0.470	0.590	
198 → 199g	246.46	A	50.61	1.403	50.1 (20)
	317.06	A	51.23	1.842	
	493.74	A	49.52	0.997	
	542.96	A	48.94	2.198	

Table 4: Results from the CLICIT experiment.

To account for this, a weighted average was taken such that the value of the χ^2 of a result is proportional to the weight given to that result. Results with excessively high χ^2 are effectively left out of the average.

The uncertainties in the least significant digits are indicated in parenthesis. The sources of this uncertainty are discussed in Section 3.5.

3.2 Cadmium-Enclosed Rabbit Results

As with the CLICIT results above, the only the resonance integral results are shown for the Cd-enclosed rabbit. These results are shown in Table 5.

Once a resonance integral result can be concluded from these and the CLICIT data, these values are used in Equation 4 to help calculate the thermal cross section from the rabbit and thermal column data.

Interaction	Gamma (keV)	Run	Resonance Integral (Barns)	χ^2 /Degrees of Freedom	Weighted Average (Barns)
190 \rightarrow 191	359.9	D	102.11	0.344	104.0 (185)
	409.44	D	107.81	1.132	
	538.91	D	106.21	1.104	
194 \rightarrow 195m	98.88	B	4.32	1.113	4.39 (28)
		C	4.39	0.651	
		D	4.49	1.521	
	129.77	C	4.36	1.370	
		D	4.54	0.499	
196 \rightarrow 197g	192.36	C	7.04	1.229	7.07 (75)
		D	6.99	0.737	
	268.71	C	7.32	1.89	
196 \rightarrow 197m	279.11	A	0.449	0.430	0.417 (19)
		B	0.450	1.167	
	346.81	A	0.309	1.387	
		B	0.395	0.909	
198 \rightarrow 199g	493.74	A	49.84	2.087	49.1 (20)
		B	48.51	2.469	
	542.96	A	49.87	3.397	
		B	48.32	2.528	

Table 5: Results from the Cd-enclosed rabbit experiment.

It is clear that there is some systematic disparity between these (Table 5) and the CLICIT results. There is a consistent difference between the two facilities that seems to depend on atomic weight. The CLICIT results are consistently larger and ranges from a ~30% difference (190 \rightarrow 191) to a

negligible difference (198 → 199g). This discrepancy is also seen in experiments on Hg and Cd by others using the same facilities.

The consistent presence of the difference suggests a systematic error. The TRIGA reactor at Oregon State University was refueled in 2008 with low enriched Uranium (LEU) fuel for proliferation reasons. According to Robert Schickler, a senior reactor operator who has been researching the neutron flux since the 2008 refueling, flux distributions appear to be different in different core locations. The refueling changed the number and distribution of active fuel rods within the core, which would affect the flux levels in different locations.

In order to measure resonance integrals, it is assumed that the epithermal flux in the reactor is proportional to $E^{-(1+\alpha)}$, where α is assumed to be close to zero. However, due to the characteristics of the core post-refueling, the effective value of α may be significantly different in different reactor locations. If the distribution of epithermal flux is different at the CLICIT and Rabbit, the resonance integral measured in each facility could be different. This may be the source of the error. Mr. Schickler is currently studying the distribution of flux in the core.

3.3 Non Cadmium-Enclosed Rabbit Results

Pt samples irradiated in the non Cd-enclosed lined rabbit were bombarded by neutrons in both the thermal and epithermal regions, allowing measurement of the thermal cross section. The resonance integrals from the Cd-enclosed rabbit results were taken and used in the calculations of the thermal cross sections. The results are presented in Table 6.

Interaction	Gamma (keV)	Run	Thermal Cross Section (Barns)	χ^2 /Degrees of Freedom	Weighted Average (Barns)
190 → 191	172.2	C	115.65	0.479	113.2 (201)
		E	105.18	0.718	
	359.9	C	120.09	0.929	
		E	111.69	0.600	
	409.4	C	116.36	2.281	
		E	110.42	0.841	
538.9	E	116.78	1.121		
194 → 195m	98.9	B	0.070	1.100	0.071 (4)
		C	0.074	1.799	
		E	0.071	0.724	
	129.8	B	0.134	0.942	
		C	0.071	0.700	
		E	0.075	1.093	
196 → 197g	192.4	B	0.71	1.744	0.72 (8)
		C	0.72	2.253	
		E	0.46	0.718	
	268.7	B	0.94	0.611	
		C	0.73	1.607	
196 → 197m	279.1	B	0.036	1.124	0.031 (1)
	346.8	A	0.028	1.100	
		B	0.031	0.659	
198 → 199g	493.7	A	3.53	1.629	2.75 (11)
		B	2.47	1.706	
	543.0	A	3.52	2.184	
		B	2.24	0.778	

Table 6: Results from the normal rabbit experiment, without Cd-enclosure.

3.4 Thermal Column Results

The TC samples were also bombarded by thermal and epithermal neutrons. Resonance integral results from both the CLICIT and Cd-enclosed rabbit were used in the calculations. It is worth noting, however, that the epithermal flux at the TC is relatively small (see Table 2), therefore the resonance integral results used for calculations have little impact on the TC thermal cross section results. These results are presented in Table 7.

Interaction	Gamma (keV)	Run	Thermal Cross Section (Barns)	χ^2 /Degrees of Freedom	Weighted Average (Barns)
190 \rightarrow 191	359.9	A	102.63	0.502	108.6 (193)
		B	104.25	0.408	
		C	110.64	1.132	
		D	111.42	1.574	
	409.4	A	108.37	0.841	
		B	112.11	1.049	
		D	108.80	1.605	
	538.9	B	111.85	0.878	
		C	113.46	0.549	
D		112.80	1.579		
194 \rightarrow 195m	98.9	A	0.055	0.977	0.059 (4)
		B	0.060	1.764	
		C	0.059	0.164	
	129.8	C	0.112	1.150	
196 \rightarrow 197g	192.4	A	0.70	5.294	0.75 (8)
		B	0.67	0.668	
		C	0.67	0.584	
		D	0.65	1.509	
	268.7	A	0.89	1.301	
		B	0.88	1.327	
C		0.94	1.849		
196 \rightarrow 197m	279.1	A	0.033	0.563	0.029 (1)
		B	0.024	2.674	
	346.8	A	0.029	1.371	
		B	0.020	12.300	
		C	0.025	1.330	
198 \rightarrow 199g	317.1	A	2.658	1.536	2.52 (10)
		B	3.031	4.330	
	493.7	A	2.46	0.953	
		B	2.45	1.263	
	543.0	A	2.54	0.955	
		B	2.46	0.715	

Table7: Results from the thermal column experiment.

The thermal cross section results from the rabbit and TC agree very well. There is no apparent disparity between the two facilities, as seen in the resonance integral measurements. The neutron flux of the rabbit and TC is mostly thermal (by factors of 24 and 425 respectively), and it is reasonable to make the assumption that the thermal flux is proportional to E^{-1} .

3.5 Uncertainty Calculations

There is a variety of sources for (non-systematic) uncertainty. These error sources are tabulated in Table 8. The uncertainty in the isotopic abundance comes from the Commission on Isotopic Abundances and Atomic Weights [2]. Although it is possible to measure the isotopic makeup of a sample to a high degree of accuracy, there can be natural variations in sample compilation depending on where in the world it was collected. CIAAW recommends using 16% uncertainty for the abundance of Pt-190 because it can vary greatly from sample to sample. Because of this, the cross section of $190 \rightarrow 191$ cannot be measured to the same accuracy as the others.

It is also worth noting that the branching ratio of the 279 keV gamma ray (for $196 \rightarrow 197m$) has an uncertainty of 25%. The other gamma ray for $196 \rightarrow 197m$ (347 keV) has much less error, so only 347 keV data was used to calculate the $196 \rightarrow 197m$ cross sections.

	190 → 191	194 → 195m	196 → 197g	196 → 197m	198 → 199g
Detector Efficiency	1%	2%	1%	1%	1%
Isotopic Abundance[2]	16%	1%	1%	1%	2%
Mass	0.50%	0.50%	0.50%	0.50%	0.50%
Half-life	1%	0.10%	0.01%	0.2%	1%
Branching Ratio	7%	5%	10%	3%	1%
Epithermal Flux	3%	3%	3%	3%	3%
Thermal Flux	3%	3%	3%	3%	3%
RI into sigma	~0%	0.6%	0.07%	0.09%	0.13%

Table 8: Non-systematic sources of error.

4 DISCUSSION

4.1 Previous Results

It is important to compare results from this experiment to the values presented in the literature. Tables 9 and 10 present literature values for Pt isotope resonance integral and thermal cross section respectively.

Mughabghab's work, *Atlas of Neutron Resonances*, is the most complete and contains values for all elements with 100 protons or fewer. The values he presents are sometimes based on calculations, original research, or are culled from previous literature results. Occasionally he will simply present values measured by R.E. Heft, whose work in the field is prolific.

	190 → 191	194 → 195m	196 → 197g	196 → 197m	198 → 199g
Mughabghab 2006 [5]	72 (10)	1.0 (1)	7.1 (3)	0.35 (7)	62 (2)
R.E. Heft 1978 [6]	67 (5)	5.13 (20)	5.56 (40)		63.6 (24)
R. Van Der Linden 1974 [7]			8 (2)		52 (3)
Hayodom 1969 [8]					55.3
P.W.De Lange 1968 [9]					50 (6)

Table 9: Previous resonance integral measurements from the literature in units of barns.

	190 → 191	194 → 195m	196 → 197g	196 → 197m	198 → 199g
Mughabghab 2006 [5]	152 (4)	0.036 (4)	0.58 (3)	0.044 (4)	3.61 (11)
H. Pomerance 1955 [10]	90 (200)	1.2 (9)	0.7 (7)		4.0 (5)
R.E.Heft 1978 [6]	152 (4)	0.036 (4)	.397 (10)		3.17 (6)
V.P. Vertebyy 1975 [11]		1.2 (4)	0.3 (2)		4.2 (3)
S.K. Mangal 1963 [12]		0.2		.069 (14)	
M. Sehgal 1962 [13]		.087 (13)	0.73 (12)	0.05 (1)	
W.A. Brooksbank 1955 [14]			0.86 (9)		
L. Seren 1947 [15]			1.1 (2)		3.92 (80)
T.B. Ryves 1971 [16]			0.74 (8)		3.66 (19)

Table 10: Previous thermal cross section measurements from the literature in units of barns.

4.2 Pt-190 → Pt-191 Cross Section

The resonance integral for this absorption was measured as 137.1 (244) b and 104.0 (185) b by the CLICIT and Cd-enclosed rabbit respectively. This is a major discrepancy with the two literature values, 72 (10) b^[5] and 67 (5) b^[6].

The thermal cross section result is 110.9 (197) b. The only two literature values are 152 (4) b^[6] from 1978 and 90 (200) b^[10] from 1955, the latter of which can obviously be ignored.

The results from this experiment do not match well with the literature. However, values presented by Heft and Mughabghab have very flawed uncertainty. The relative abundance of Pt-190 is extremely low, and the CIAAW recommends a 16%, while the overall uncertainty claimed by Heft is as low as 2.6%.

4.3 Pt-194 → Pt-195m Cross Section

The resonance integral was measured as 5.10 (32) b and 4.39 (28) b in the CLICIT and Cd-enclosed rabbit respectively. This agrees very well with Heft's value (5.13 (20) b^[6]), but Mughabghab's value (1.0 (1) b^[5]) is much different.

For the thermal cross section, our measurement of 0.065 (4) b agrees fairly well with Sehgal's measurement of 0.087 (13)b^[13]. The other values presented in the literature vary widely, by as much as 3000%. It is worth noting that Sehgal's other thermal cross section measurements (for 196 → 197g and 196 → 197m) also agree well with ours.

4.4 Pt-196 → Pt-197g Cross Section

For Pt-196 → Pt-197g, the CLICIT resonance integral result is 8.52 (90) b, while the Cd-enclosed rabbit is 7.07 (75) b. The previous literature matches these values very well (7.1 (3) b^[6], 5.56 (40) b^[5], 8 (2) b^[7]).

Our thermal cross section value for Pt-196 → Pt-197g is 0.74 (8) b, with several literature values coming very close (0.73 (12) b^[13], 0.74 (8) b^[16]) and the rest within the same range.

Heft's values, which are usually reliable, are smaller than the values presented here and in the literature. This is mostly because he used 0.057 for the branching ratio of the 192 keV gamma; the actual branching ratio is 0.037. It is unclear whether this is a mistake or the branching ratios have simply become better known over time.

4.5 Pt-196 → Pt-197m Cross Section

Our resonance integral results for Pt-196 → Pt-197m are 0.497 (22) b and 0.417 (19) b for the CLICIT and Cd-enclosed rabbit respectively. The only value presented in the literature is Mughabghab value of 0.35 (7) b^[5]. It is unclear where he got this value. It may be a measurement or a theoretical value.

The thermal cross section value is 0.030 (1) b. The other literature values don't agree very well with us or each other, but all values are within a factor of two.

5.6 Pt-198 → Pt-199g Cross Section

Unlike the other resonance integral measurements, the values for the Pt-198 → Pt-199g as measured by the CLICIT and the Cd-enclosed rabbit agree very closely. This value is 49.6 (20) b. This agrees

well with the literature, with Mughabghab and Heft's values skewing slightly higher (62 (2) b^[5], 63.6 (24) b^[6]).

The thermal cross section for Pt-198 \rightarrow Pt-199g was 2.64 (11) b. This is significantly less than the literature values, which are around 3.5 to 4 barns. However, it is unclear whether or not these measurements took into account the production of 199g atoms from the 199m isomer. Since 199m has a half-life of 13.6 seconds, virtually all 199m atoms will transition to the ground state by the time sample decay is measured. This would make the activity greater and the cross section would appear larger.

5 CONCLUSION

The purpose of this experiment was to quantitatively measure the thermal cross section and epithermal resonance integral – which together make up the total neutron absorption cross section – of the stable platinum isotopes that emit gamma radiation upon decay. Pure, natural platinum foil samples were bombarded by neutrons produced by Oregon State University’s TRIGA reactor. After activation, the excited samples were placed in front of high purity Germanium (HPGe) photon detectors to count characteristic photons. These counts were used to calculate the sample activities for each isotope, which were used – along with the neutron flux levels and the reaction rate equation – to calculate the cross sections.

The neutron absorption cross section is an important material property that can affect the way the material is used and how it behaves in technological applications. Previous measurements of the Pt cross sections are not convincing. For a variety of reasons, the literature values vary widely. Many of the measurements were made decades ago, when characteristic gamma branching ratios, natural isotopic abundances, and half-lives were less accurately known. Some of these values have changed by factors of two in the last few decades. Current HPGe detector technology allows unprecedented energy spectra resolution, which increases counting accuracy significantly.

Furthermore, few – if any – past experiments have measured all Pt cross sections simultaneously, using different multiple independent reactor facilities. This allows us to uncover biases due to inconsistencies in the distribution of neutron flux in the reactor, which we detected in this experiment and has also been detected in other similar experiments with different elements irradiated in the same reactor core. In broad-spectrum neutron activation analysis, the assumption must be made that neutron flux in the core is only a function of neutron energy, but in reality this is not the case. Using different reactor facilities revealed a systematic difference between resonance integrals measured in two of the locations, most likely due to flux inconsistencies. Currently, research is being done by the TRIGA staff to better understand the flux distributions in the core. Additional iterations of the experiment are planned at OSU to probe these differences.

6 ACKNOWLEDGEMENTS

I would like to acknowledge Dr. Ken Krane, who led this research project and has been measuring cross sections for years. Without his help, this thesis would not have been possible. I would also like to thank the helpful staff of the OSU TRIGA reactor, who performed our irradiations.

7 REFERENCES

- [1] Los Alamos National Laboratory. (1998, May 5). *Nuclear Reactions*. Retrieved May 16, 2012, from <http://t2.lanl.gov/tour/sch002.html>
- [2] Berglund, M., & Wieser, M. E. (2011, January 14). *Commission on Isotopic Abundances and Atomic Weights*. Retrieved from <http://ciaaw.org/pubs/TICE2009.pdf>
- [3] Brookhaven National Laboratory. (n.d.). *Chart of Nuclides*. Retrieved 2012, from National Nuclear Data Center: <http://www.nndc.bnl.gov/chart/>
- [4] Oregon State University. (2005). *Radiation Center*. Retrieved May 16, 2012, from Oregon State University: <http://radiationcenter.oregonstate.edu/index.html>
- [5] Mughabghab, S. F. (2006). *Atlas of Neutron Resonances Fifth Edition*. Oxford: Elsevier Science.
- [6] Heft, R. (1978). A Consistent Set of Nuclear-Parameter Values For Absolute Instrumental Neutron Activation Analysis. *Proceedings of the International Conference on Computer in Active Analysis*.
- [7] Van Der Linden, R., De Corte, F., & Hoste, J. (1974). A Compilation of Infinite Dilution Resonance Integrals, II. *Radioanalytical Chemistry*, 20133-141.
- [8] Hayodom et al., (1969). Resonance Integral Measurements. *Thai-AEC 23 Progress Report, Thailand*.
- [9] de Lange, P., & Bigham, C. (1968). Multi-Element Detectors For Activation Resonance Integral and Resonance Spectrum Measurements. *Nuclear Applications*, 190-95.
- [10] Pomerance, H. (1955). Absorption Cross Section For Long-Lived Fission-Product Zr-93, Am-241, and Enriched Stable Platinum Isotopes. *Neutron Cross Sections and Fission Physics*, 50-56.
- [11] Vertebnyy, V., Vorona, P. N. et al., (1975). Interaction of the Slow Neutrons With the Osmium and Platinum Isotopes. *Yadernaya Fizika*, 22, 674.

- [12] Mangal, S., & Gill, P. (1963). Thermal Neutron Activation Cross-Sections For Isomer Production Part II. *Nuclear Physics*, 41, 542.
- [13] Sehgal, M. (1962). Isomeric Cross-Section Ratios in (n, gamma) Reactions. *Physical Review*, 128, 761-67.
- [14] Brooksbank, W., Leddicotte, G. et al., (1955). Slow Neutron Activation Cross Sections of Several Elements, *Nuclear Engineering and Science Congress*, Cleveland, OH, Dec. 12-16.
- [15] Seren, L., Friedlander, H., & Turkel, S. (1947). Thermal Neutron Activation Cross Sections. *Physical Review*, 72, 888–901.
- [16] Ryves, T. (1971). Further Activation Thermal Neutron Capture Cross-Sections and Resonance Integrals. *Journal of Nuclear Energy*, 25, 35–42.